Water Research 227 (2022) 119296

Contents lists available at ScienceDirect

Water Research

journal homepage: www.elsevier.com/locate/watres

# Removal of small elemental sulfur particles by polysulfide formation in a sulfidic reactor

Annemerel R. Mol [a,b,*], Sebastian D. Pruim [a], Milan de Korte [c], Derek J.M. Meuwissen [a], Renata D. van der Weijden [a,d], Johannes B.M. Klok [a,b,d], Karel J. Keesman [c,d], Cees J.N. Buisman [a,d]

[a] Environmental Technology, Wageningen University & Research, P.O. Box 17, 6700 AA, Wageningen, the Netherlands
[b] Paqell B.V, Reactorweg 301, 3542 CE Utrecht, the Netherlands
[c] Mathematical and Statistical Methods - Biometris, Wageningen University and Research, P.O. Box 16, 6700 AA Wageningen, the Netherlands
[d] Wetsus, European Centre of Excellence for Sustainable Water Technology, P.O: Box 1113, 8900 CC Leeuwarden, the Netherlands

ARTICLE INFO

*Keywords:*
Biological desulfurization
Elemental sulfur
Particle size
Polysulfide
Sulfide

ABSTRACT

For over 30 years, biological gas desulfurization under halo-alkaline conditions has been studied and optimized. This technology is currently applied in already 270 commercial installations worldwide. Sulfur particle separation, however, remains a challenge; a fraction of sulfur particles is often too small for liquid-solid separation with conventional separation technology. In this article, we report the effects of a novel sulfidic reactor, inserted in the conventional process set-up, on sulfur particle size and morphology. In the sulfidic reactor polysulfide is produced by the reaction of elemental sulfur particles and sulfide, which is again converted to elemental sulfur in a gas-lift reactor. We analyzed sulfur particles produced in continuous, long term lab-scale reactor experiments under various sulfide concentrations and sulfidic retention times. The analyses were performed with laser diffraction particle size analysis and light microscopy. These show that the smallest particles (< 1 μm) have mostly disappeared under the highest sulfide concentration (4.1 mM) and sulfidic retention time (45 min). Under these conditions also agglomeration of sulfur particles was promoted. Model calculations with thermodynamic and previously derived kinetic data on polysulfide formation confirm the experimental data on the removal of the smallest particles. Under the 'highest sulfidic pressure', the model predicts that equilibrium conditions are reached between sulfur, sulfide and polysulfide and that 100% of the sulfur particles <1 μm are dissolved by the (autocatalytic) formation of polysulfides. These experiments and modeling results demonstrate that the insertion of a novel sulfidic reactor in the conventional process set-up promotes the removal of the smallest individual sulfur particles and promotes the production of sulfur agglomerates. The novel sulfidic reactor is therefore a promising process addition with the potential to improve process operation, sulfur separation and sulfur recovery.

## 1. Introduction

Sulfur is the 10th most abundant element in the universe and plays a vital role in the Earth's ecosystem through the (bio)chemical sulfur cycle (Palme et al., 2014). The element can be present in various oxidation states, from sulfide ($S^{2-}$) being the most reduced state (−2) to sulfate ($SO_4^{2-}$) being the most oxidized state (+6). Elemental sulfur (S with an oxidation state of zero), can be recovered from (bio)gas streams using biological desulfurization (BD). Sulfur is present in this (bio)gas as toxic and corrosive $H_2S$. By removing $H_2S$, corrosion of pipes, toxicity to humans and the ecosystem and the generation of acid rain are prevented (Guidotti, 2010; Likens and Bormann, 1974; Pope et al., 2007; Smith et al., 2011). Main advantages of BD in comparison with chemical and physical alternatives are operation at ambient pressure and temperature, and without toxic chemicals (Cline et al., 2003; Van Den Bosch et al., 2007). In BD under halo-alkaline conditions, $H_2S$ present in sour gas (gas with substantial amounts of $H_2S$) is absorbed in a moderately alkaline solution, reacts to soluble bisulfide and is subsequently oxidized in a gas-lift reactor by a mixed culture of sulfide-oxidizing bacteria (SOB) to elemental sulfur (Eq.1)

* Corresponding author.
*E-mail address:* annemerel.mol@wur.nl (A.R. Mol).

https://doi.org/10.1016/j.watres.2022.119296
Received 15 August 2022; Received in revised form 22 October 2022; Accepted 25 October 2022
Available online 25 October 2022

$$HS^- + 1/2O_2 \rightarrow S^0 + OH^- \quad (1)$$

At ambient temperatures and pressures elemental sulfur exists in rings and polymeric chains of different sizes ($S_n$). In BD under halo-alkaline conditions, eight $S^0$ atoms form a ring ($S_8$) and crystallize to the most stable configuration in aqueous systems which is orthorhombic α-$S_8$ (Mol et al., 2020). Next to formation of elemental sulfur, oxidized by-products such as sulfate and thiosulfate are formed due to over-exposure to dissolved oxygen. Sulfate is formed biologically while thiosulfate is formed abiotically. These compounds are undesirable as they lead to acidification and consequently addition of chemicals is needed to neutralize the process solution. Moreover, elemental sulfur is the preferred S-species as it is stable, easy to separate, transport, store and re-use due to its solid properties. Biologically produced sulfur is known to have hydrophilic properties, which makes it more suitable for applications in water in comparison with chemically produced sulfur (Janssen et al., 2009). In this study, we further refer to elemental sulfur as 'sulfur', describing the solid, elemental material.

Although BD under halo-alkaline conditions has been intensively studied and is already largely applied on a commercial scale (>270 installations worldwide in 2017) (Buisman et al., 1990; De Rink et al., 2019; Janssen et al., 1999; Kiragosyan et al., 2019; Klok et al., 2017, 2013, 2012; Van Den Bosch et al., 2007), the sulfur settleability is still a major challenge. In recent years the scale of BD installations has increased due to their application for natural gas desulfurization. This trend makes certain operational parameters, such as sulfur separation, even more important. Even though sulfur separation in larger installations often happens with a decanter centrifuge or hydrocyclone, a concentration step of the reactor suspension before entering the centrifuge is still beneficial for operation of the centrifuge. For smaller installations a centrifuge is often not economically viable, so sulfur separation relies solely on the settleability of the sulfur particles. Due to the lack of control over sulfur particle properties, such as size and morphology, the sulfur particles sometimes settle poorly. In this study, we use the term 'particle' as an umbrella term, including colloids, crystals, intergrown crystals, aggregates, agglomerates etc. unless otherwise specified. In this case, a particle is any shape the elemental sulfur can take, as long as in a sedimentation context it settles as one unit. Differences in settleability between various industrial reactors were found in an earlier study (Mol et al., 2020). In this earlier study, we described that small, non-settling sulfur particles with a median diameter of 0.3 μm could account for at least 13.6% of the total number of particles. Additionally, it was reported that in industrial BD installations settleability of the produced sulfur can fluctuate over time (L. Feenstra, Industriewater Eerbeek, personal communication, 7 September 2021). Poorly settleable sulfur may lead to hampered process operation, as it accumulates in the system. Accumulated sulfur can cause clogging of pumps and pipes, and, under high concentrations, foaming as well (Kleinjan et al., 2006). Moreover, small sulfur particles are more prone to side reactions, such as oxidation, due to their larger relative surface area. Another reason why sulfur needs to be recovered effectively is that sulfur as raw material is expected to become more important in the future. Not only is sulfur an essential nutrient for agriculture, but there is also an emerging market for sulfur in other applications such as capacity cathode material in rechargeable batteries, advanced materials, metal bioleaching or as electron donor in autotrophic denitrification (Di Capua et al., 2016; Eriksen et al., 2004; Florentino et al., 2015; Lim et al., 2015; Roig et al., 2004; Seidel et al., 2006; Soares, 2002; Ucar et al., 2020; Zhu et al., 2019). Therefore, it is relevant to improve sulfur recovery.

Sulfur particle recovery is a challenge. As a solution, we propose a new process design to remove the smallest particles (< 1 μm) from the reactor liquid. This new design was used in two earlier studies, but with a different experimental purpose (De Rink et al., 2019; Kiragosyan et al., 2020). The design consists of a sulfidic reactor in which the smallest sulfur particles are dissolved to polysulfides by a reaction with sulfide. The formed polysulfides can then again be (biologically) oxidized to elemental sulfur upon exposure to oxygen in the gas-lift reactor. The sulfidic reactor is placed between the absorber and the gas-lift reactor and the reactor content (buffered medium, SOB, sulfur particles, dissolved sulfur species) is continuously circulated over all reactor compartments of the set-up. The retention time in the absorber and sulfidic reactor can be called 'Sulfidic' Retention Time (SuRT). SuRT is defined as the amount of time the reactor content is retained under sulfidic, anoxic conditions before being pumped to the gas-lift reactor.

In this study, we have investigated the effect of various Total Dissolved Sulfide (TDS) concentrations and SuRTs on the presence of sulfur particles with a diameter <1 μm in the solution. This was tested by long term, continuous, lab-scale bioreactor experiments. The results were validated with a model based on physical and chemical laws, describing the effect of TDS concentration and SuRT on polysulfide formation rates and particle dissolution.

## 2. Materials and methods

### 2.1. Experimental set-up

A lab-scale reactor set-up was used with an absorber (A) and gas-lift reactor (C) (Fig. 1). For extended configuration, two additional reactor compartments were added: a sulfidic reactor (B) between the absorber and the gas-lift reactor and a settler (D) after the gas-lift reactor. Reactor A had a height of 27 cm and an inner diameter of 4.5 cm, reactor B had a height of 75 cm and inner diameter of 12.5 cm, reactor C had a height of 85 cm and inner diameter of 12.5 cm, and reactor D had a height of 55 cm and upper inner diameter of 10 cm and bottom inner diameter of 3.2 cm. Reactor A was not stirred but mixed by the liquid in-and outflows. Reactor B was mechanically stirred with a stainless-steel stirrer. Reactor C was a gas-lift reactor which was stirred by the downer-riser flows created by the introduction of gas in the bottom of the reactor. The inner column was 8 cm in diameter and had a height of 44.5 cm. Reactor D was not stirred. The sulfidic reactor is a zone with retention time of reactor content (buffered medium, SOB, sulfur particles, dissolved sulfur species) under anoxic, (poly)sulfidic pressure. The absorber by itself is also a small sulfidic zone. The liquid volumes of the set-ups with and without the sulfidic reactor were 9.1 and 5.6 L, respectively (both with settler). Without settler (but with sulfidic reactor) the wet volume was 7.6 L. The volume of the gas-lift reactor was 3.7 L. The gas flow was recycled over the headspace of gas-lift reactor with a vacuum pump to prevent any release of the $H_2S$ gas and to reach low oxygen concentrations. The gas was introduced with a porous stone to the bottom of the inner column of the gas-lift reactor to ensure proper oxygen transfer and mixing. Pure $H_2S$ gas and oxygen were supplied by mass flow controllers (Brooks, 5850E series, 0–100 nml/min and 0–20 nml/min for oxygen and $H_2S$ during the experiment with the middle and lowest $H_2S$ loading, Brooks Instrument LLC, Hatfield, USA). In case of pressure build-up, excess gas was discharged via a water-lock saturated with zinc acetate to capture any potentially present $H_2S$. The reactors were operated at 35 °C using a thermostat bath and climate-controlled cabinet.

### 2.2. Medium composition

The medium consisted of a buffer with 6.6 g $L^{-1}$ $Na_2CO_3$ and 69.3 g $L^{-1}$ $NaHCO_3$ in demineralized water at pH 8.5. Fresh buffer was supplied at a constant flow to maintain enough alkalinity in the system. Furthermore, a nutrient stock was supplied for biological growth containing (in g per 1 L of demineralized water): $K_2HPO_4$, 0.1; $MgCl_2$ $6H_2O$, 0.0203; NaCl, 0.6; $CH_4N_2O$, 0.06 and 2 mL $L^{-1}$ trace element solution as in Pfenning and Lippert (Pfennig and Lippert, 1966).

### 2.3. Experimental operation

The experiments carried out with the various conditions are numbered Exp. 1–4. An overview of the operational conditions per

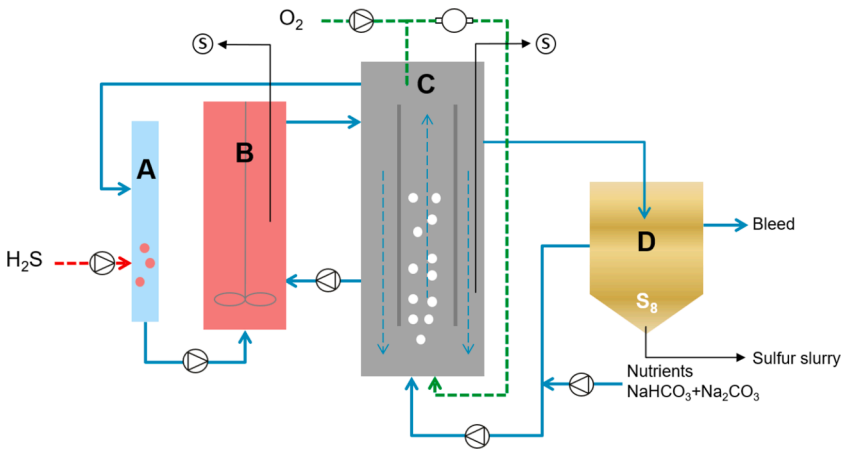


**Fig. 1.** Experimental set-up. A) absorber, B) sulfidic reactor, C) gas-lift reactor, D) settler and S) sampling port. For the line-up without the sulfidic reactor, the liquid from the absorber was introduced in the bottom of the gas-lift reactor. For the line-up without the settler, the solution was recirculated through the connection where nutrients and medium were added. Dashed lines are gas streams. Solid lines are liquid streams.

experiment is provided in Table 1. A settler was included for the experiments with the highest $H_2S$ loading rate to prevent sulfur accumulation in the system, i.e. to avoid operational issues such as foaming and clogging due to sulfur build-up. Experiments with lower $H_2S$ loading rate were conducted without the settler to collect a sample in which all particles that were produced under the specific experimental conditions were present, without removing any particles with the settler. We assume that the removal of the largest, settling particles does not impact the presence of the smallest particles in the process solution. The latter is studied in this paper. Reactors were filled with medium and inoculated. In all experiments, the set-up was operated in continuous mode without interruption. Throughout all experiments, the $H_2S$ supply was kept constant for that experiment. The $H_2S$ load was used to set the TDS concentration in the sulfidic reactor. To keep the conversion efficiency from sulfide to sulfur high, the oxidation–reduction potential (ORP) was set at −360 mV vs. Ag/AgCl, which is a representative set-point for industrial reactors. The ORP set-point was controlled by a proportional-integral (PI) controller. The PI controller regulated the oxygen supply rate. Samples (well-mixed reactor content with sulfur particles, medium and microorganisms) were taken for analysis at a sampling port in the middle of the sulfidic reactor (Exp. 3–4) and the gas-lift reactor (all experiments). The sampling tubes from the reactor were flushed three times prior to sampling to obtain a representative sample.

### 2.4. Inoculum

Exp. 1 was inoculated with centrifuged microorganisms (to remove excess sulfur) from a lab-scale sulfur-producing gas-lift bioreactor, operated under continuous conditions, like the conditions applied in this experiment. The original inoculum of this reactor was obtained from a well-characterized industrial scale BD facility under halo-alkaline conditions of Industriewater Eerbeek B.V. (Eerbeek, The Netherlands, hereafter referred to as 'Eerbeek') (Janssen et al., 2009). To remove the sulfur, the reactor content was centrifuged at 4500 RPM for 20 min (FirLabO, Froilabo, Paris, France). A pellet was formed with two layers: a bottom layer of elemental sulfur and a layer with microorganisms on top. The layer with microorganisms was carefully washed off. Exp. 4 was inoculated with centrifuged microorganisms directly taken from Eerbeek. Exp. 2 and 3 were inoculated with microorganism-rich process solution from Exp. 1 and 4 as described in Table 1.

**Table. 1**
Experimental conditions.

| Process condition | Exp. 1 | Exp. 2 | Exp. 3 | Exp. 4 |
|---|---|---|---|---|
| Sulfidic reactor | no | yes | yes | yes |
| Sulfidic retention time (min) | 4.8 | 45.0 | 38.7 | 38.7 |
| TDS concentration in sulfidic zone (mM) | 8.3 | 4.4 | 1.9 | 1.0 |
| S-loading rate (g S $L^{-1}$ gas-lift reactor $day^{-1}$) | 4.4 | 4.4 | 2.0 | 1.0 |
| Total system volume [a] (L) | 5.6 | 9.1 | 7.6 | 7.6 |
| Duration (days) | 31 | 28 | 16 | 41 |
| Inoculum | Enriched from Eerbeek in lab-scale reactor | Exp. 1 | Exp. 4 | Eerbeek |

[a] Volumes of reactor compartments can vary slightly.

### 2.5. Analysis

Reactors were equipped with sensors for temperature and ORP (Triple Junction, platinum rod, glass electrode equipped with an internal Ag/AgCl reference electrode, ProSense, Oosterhout, The Netherlands). Methods to measure sulfate and thiosulfate concentrations, sulfur particle size distribution (PSD), alkalinity, conductivity, pH and total sulfur concentration were previously described elsewhere (Mol et al., 2020). PSD can be expressed both volumetrically and numerically; in a volumetric based particle size distribution, larger particles have a heavier weight as, due to their size, they often comprise a larger percentage of the total solid volume. In a numeric based distribution, each particle has an equal weight, independent of the particle size. According to common practice, when a PSD had to be represented by a single value, the median (D50) of the PSD was reported to show the particle size development over time. The median has a better way of representing the central location of the data in a non-normal distribution than the mean and is relatively unaffected by outliers (Field, 2009) .

The microorganism concentration was measured as the amount of total nitrogen as in De Rink et al. (2019). This method is based on the absorbance of nitrophenol at 345 nm and performed with the TNTplus™ 826 persulfate digestion method (Hach Company, Loveland, Colorado, United States). Presence of biologically produced sulfur did not affect the measured nitrogen concentration (Van Den Bosch et al., 2007). Analysis of sulfur particles with light microscopy was performed according to Mol et al. (2020). Process selectivity for elemental sulfur was calculated by the mass balance based on $H_2S$ supply and the measurement of dissolved sulfur products formed (De Rink et al., 2019). In our study when the term '$HS^-$' is used, we refer to the sum of TDS ($H_2S$, $HS^-$ and $S^{2-}$) as most of the dissolved sulfide is present as $HS^-$ at pH 8.5. Operational reactor data can be found in SI Table 1.

### 2.6. Mathematical model

A mathematical model of a continuous stirred-tank reactor (CSTR) was developed to simulate the polysulfide formation in the sulfidic zone of the experimental setup. It is assumed that this zone is ideally mixed, i.e. pH and temperature are constant. The mass balances, in terms of a set of differential equations, are given by:

$$\frac{dC_s}{dt} = \frac{Q}{V}\cdot\left(C_{S,in} - C_S\right) - (x-1)\cdot R_{Sx} \tag{2}$$

$$\frac{dC_{Sx}}{dt} = -\frac{Q}{V}\cdot C_{Sx} + R_{Sx} \tag{3}$$

$$\frac{dC_{HS}}{dt} = \frac{Q}{V}\cdot\left(C_{HS,in} - C_{HS}\right) - R_{Sx} \tag{4}$$

Whereby $C_s$ is the concentration of sulfur present in small sulfur particles in the sulfidic zone (Fig. 1, reactor B) (mol-S$\bullet L^{-1}$), $C_{S,in}$ the concentration of sulfur present in small sulfur particles in the feed to the sulfidic zone (Fig. 1, concentration in flow from reactor A and C to B) (mol-S$\bullet L^{-1}$), $Q$ the volume flow to the sulfidic reactor (flow from reactor A and C to B) (L$\bullet s^{-1}$), $V$ the volume of the sulfidic zone (reactor B) (L), $x$ the average chain length of polysulfide, $R_{Sx}$ the average formation rate of polysulfide (for all possible values of $x$) (mol$\bullet L^{-1}\bullet s^{-1}$), $C_{Sx}$ the concentration of polysulfide (mol$\bullet L^{-1}$), $C_{HS}$ the concentration of TDS in the sulfidic zone and $C_{HS,in}$ the concentration of TDS in the feed of the sulfidic zone (mol-S $\bullet L^{-1}$). The term '$-1$' in Eq. (2) represents the 'S' that originates from $HS^-$ in the reaction with elemental sulfur or polysulfide, and thus does not contribute to the mass balance of zero valent elemental sulfur.

While polysulfide formation is known to be a sequence of reaction steps, after which long chain polysulfides $S_9^{2-}$ can rearrange to shorter chain length, we assume for the sake of simplicity that all polysulfides that are formed have an average chain length $x$, which is calculated based on the thermodynamic expressions by Kamyshny et al. (2004). The calculated value of $x$ for the experimental conditions is 5.05, which is in agreement with reported measurements under similar conditions by Roman et al. (i.e. 5.17 and 5.18) (2014) .

The polysulfide formation rate is generally described by both uncatalyzed and catalyzed reactions, slightly adjusted from Kleinjan et al. (2005a):

$$R_{Sx} = \frac{Ac\cdot(\overline{C_{Sx}} - C_{Sx})}{C_{H+}}\cdot\left(k_1^*\cdot(\overline{C_{Sx}} - C_{Sx}) + k_2^*\cdot C_{Sx}\right) \tag{5}$$

Where $Ac$ is the concentration of the specific surface area of sulfur ($m^2\bullet m^{-3}$), $k_1^*$ and $k_2^*$ the uncatalyzed and catalyzed reaction rates respectively ($s^{-1}$), $C_{H+}$ the concentration of protons (mol $\bullet L^{-1}$) and $\overline{C_{Sx}}$ the equilibrium concentration of polysulfide (mol $\bullet L^{-1}$). The latter term is adjusted to describe the dynamic equilibrium and is obtained via the equilibrium constant for average polysulfide chain length, $Kx$, according to Kleinjan et al. (2005b):

$$\overline{C_{Sx}} = Kx\cdot\frac{C_{HS-}}{C_{H+}} \tag{6}$$

We hereby assume that the TDS concentration does not go to zero. A list with parameters is provided in the Supplementary Information (SI Table 2)

## 3. Results and discussion

### 3.1. Particle size

Four long term (16–41 days), continuous lab-scale reactor experiments were performed at different TDS concentrations and SuRTs i.e. using an additional sulfidic process step. Sulfide was successfully converted to elemental sulfur under all four applied conditions, leading to the presence of sulfur particles in the reactor solution. Operational reactor performance data on parameters such as product formation, bacteria concentration etc. can be found in SI Table 1. Particle size distributions (PSD) of sulfur particle samples at the end of each experiment taken from the gas-lift reactor during the experiments are shown in Fig. 2.

In general, the number-based particle size distributions ranged from 0.1 to 50 μm. This is a typical size distribution for biologically formed sulfur particles in these types of systems (Janssen et al., 1996; Kleinjan et al., 2005a; Leerdam et al., 2011; Li et al., 2020; Mol et al., 2020; Mu et al., 2021; Roman, 2016). The particles had a unimodal distribution, except for Exp. 3 where the distribution had a bimodal tendency. The particles from Exp. 1 had a median particle size of 0.6 μm. The particles from Exp. 2 are considerably larger with a median diameter of 3.8 μm. From previous work it is known that the peak of Exp. 2 likely belongs to sulfur agglomerates and the peaks of Exp. 1, 3 and 4 to single particles or a mix thereof (Mol et al., 2020). For the samples from Exp. 3 and 4 the median particle sizes were 0.9 and 0.7 μm respectively.

Fig. 3 provides an overview of the median particle diameters of particles from all four experiments over time. As the range on the y-axis does not allow for details to be visible for Exp. 1, 3 and 4, the same data can be found in SI Fig. 1 with a y-axis range of 0–2 μm.

The conditions in Exp. 2 were found to be optimal for the removal of the smallest particles. In this experiment the TDS concentration was relatively high in the sulfidic reactor (4.4 mM) and SuRT was the longest of all experiments (45.0 min). This combination of high TDS concertation and long SuRT lead to high 'sulfidic pressure'. During the entire experiment, Exp. 2 is dominated by larger particles (3.5 ± 1.9 μm), whereas the particles from the other experiments are considerably smaller. In Exp. 2, submicron (<1 μm) particles have almost completely disappeared. A likely explanation is that they have reacted to polysulfides. At higher TDS concentration (8.3 mM), but much shorter SuRT (4.8 min) the particles had an average median diameter of 0.3 ± 0.2 μm (Exp. 1). At a moderate TDS concentration (1.9 mM), but with similar SuRT as Exp. 2, the median particle diameter was 0.5 ± 0.2 μm (Exp. 3). The median particle diameter of Exp. 3 is thus also smaller than the median particle diameter of Exp. 2. Interestingly, the particles in Exp. 3 seemed to grow towards the end of the experiment (Fig. 4). At day 13, an elbow-shaped peak appears after 1 μm and the peak below 1 μm shifts to the right and becomes smaller. This shows that small particles are disappearing. However, at day 10, the particle size on average again became smaller. A peak appeared at 50–100 nm in one of the triplicate measurements. Possibly the particles causing this peak were freshly formed sulfur nuclei. Perhaps they were only present in smaller amounts and therefore were not measured on other PSDs, such as on day 3. On the last day, day 16, the median particle diameter was 0.9 μm. This final median particle diameter is considerably larger than average median particle diameter of Exp. 3. The hydraulic retention time (HRT) in Exp.3 was 25 days and as the set-up used in Exp. 3 did not have a settler, the

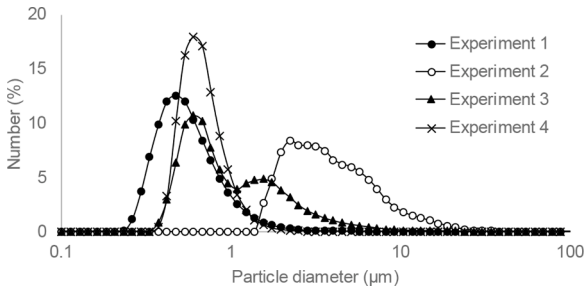


**Fig. 2.** PSD for the experiments. Samples were taken on day 28 of the respective experiment (except Exp. 3 at day 16). Lines are average of triplicate measurements with average maximum deviation of 0.9%. Exp.1 median=0.6 μm, Exp. 2 median= 3.8 μm, Exp. 3 median =0.9 μm and Exp. 4 median = 0.7 μm.

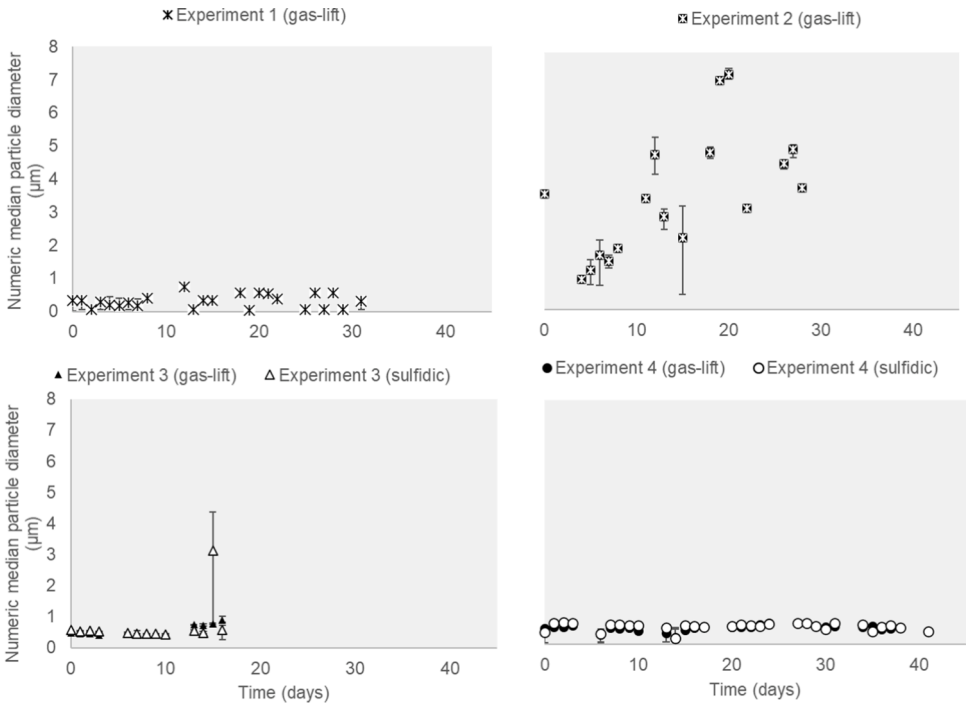


**Fig. 3.** Influence of operational parameters on median sulfur particle diameter. The median particle diameters of Exp. 1–4 were measured over the entire course of the experiments. For Exp.3–4 samples were also analysed from the sulfidic reactor. For Exp. 2 this was not done, and Exp. 1 did not have a sulfidic reactor.

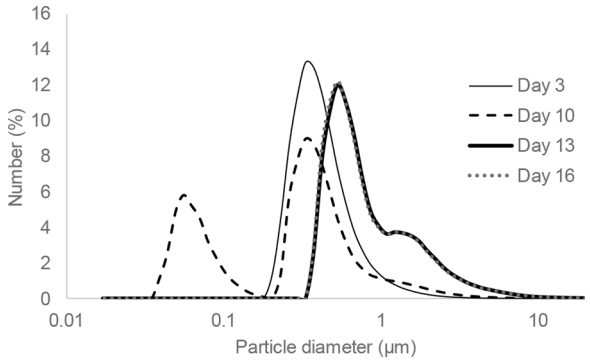


**Fig. 4.** Particle size development in Exp. 3. Particle size distributions are averages of triplicate measurements. Particles are getting bigger over time with a large shift from day 13 onwards, likely due to the dissolution of the smallest particles to polysulfides. At day 10, also a peak below 0.1 um appears in one of the triplicates. This peak could be attributed to freshly formed sulfur nuclei. Maximum deviation between triplicates day 3 = 0.2%, day 10=11.6%, day 13=1.1% and day 16=3.0%.

HRT was assumed to be equal to the retention time of particles in the set-up. The slow dynamics of the behavior of particle size along time in Exp.3 were due to this long HRT and relatively low sulfide loading rate. Interestingly, in Exp.4, which has a similar HRT of 23 days, no growth at all was observed likely due to the even lower sulfide loading rate.

In addition, in the gas-lift reactor the particles were significantly larger than in the sulfidic reactor towards the end of the experiment (see SI Fig. 1 for a figure with smaller range on y-axis). This is likely due to the partial breakdown of particles in the sulfidic reactor, which are then rebuilt due to new sulfur formation by (poly)sulfide oxidation in the gas-lift reactor. In Mol et al. (2021, 2022) the agglomeration process was studied in more detail. It was shown that the agglomerates are shaped through a balance between build-up by freshly formed particles and breakdown of particles to polysulfide. For Exp. 4, at the lowest TDS concentration (1.0 mM), the particle size remained stable throughout the experiment with a median diameter of 0.5 ± 0.1 µm, probably because the $HS^-$ concentration was limiting the dissolution of sulfur. Evidently, the addition of a sulfidic reactor leads to the removal of the smallest submicron particles if the TDS concentration is sufficiently high. It seems that Exp. 3 was operated at boundary conditions, as we observe just a slight effect on particle size, and only at the end of the experiment.

### 3.2. *Particle size and morphology analysis with light microscopy*

The sulfur particles formed under the various experimental conditions had distinctively different morphologies as observed with light microscopy (Fig. 5). Sulfur particles were distinguished in the light microscopy pictures as light, radiant particles (single particles) or darker patches with light, radiant edges (agglomerated particles). The black spots in the background were microorganisms as they showed movement and on occasion, a dividing 'black spot' was observed. Furthermore, the appearance of SOB is similar in light microscopy pictures in other publications (Marnocha et al., 2016; Sorokin et al., 2006).

In the pictures of Exp. 1 and 4, many small individual (sub)micron-sized sulfur particles were visible, which is in good agreement with the particle size distribution (Fig. 5a, d). In Exp. 1 also large agglomerates (~20 µm) were present in seemingly low concentration. The concentration was likely too low to be visible in the number-based particle size distribution. In Exp.1 and 4 the particles seemed mainly globular (rough and smooth) and around a size of 1 µm.

In Exp. 2, however, small (sub)micron particles were hardly visible (Fig. 5b). Also, in Exp. 3 not a lot of these particles seemed present, at least not as many as in Exp.1 and 4 (Fig. 5c). Larger, agglomerated, sulfur particles were observed in the pictures of Exp. 2 and 3. In both experiments large agglomerates were visible of 20–30 µm, but also smaller ones of 5–10 µm. The center of the agglomerates appeared dark due to the thickness of the sample, which could be observed while focusing the microscope. No microorganisms were observed attached to the agglomerates, as they could easily be distinguished as small black spots of around 1 µm in the sample. It is possible that due to mixing during PSD measurement, the larger aggregates were slightly broken

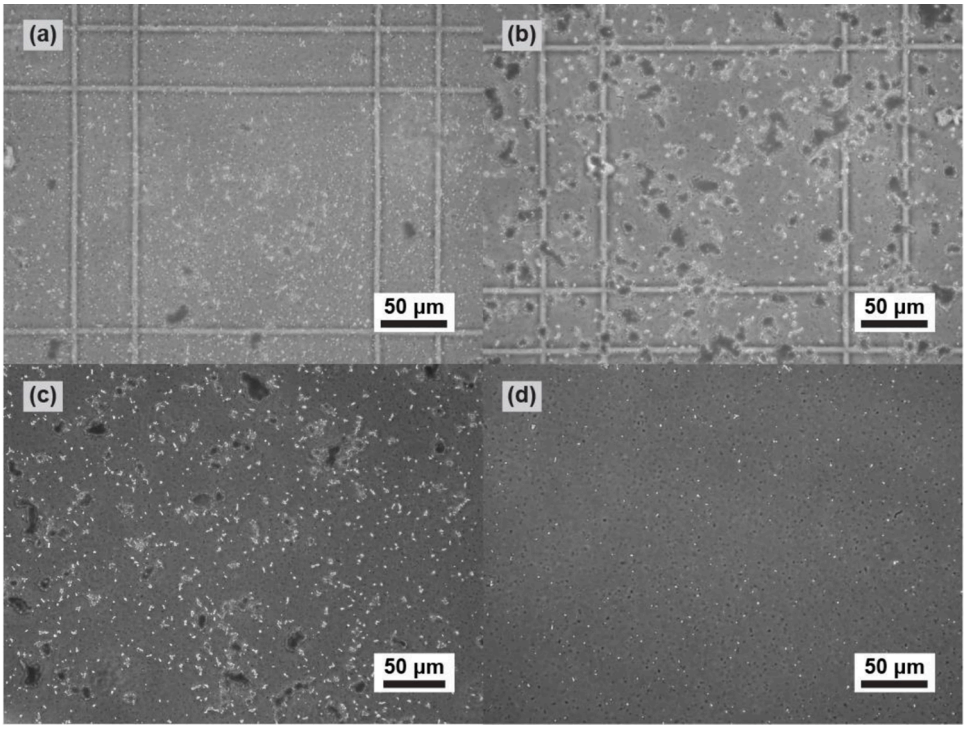


**Fig. 5.** Light microscopy pictures (400x magnification) of gas-lift reactor suspension with sulfur particles and microorganisms under different experimental conditions. a.) Exp. 1 (day 21), b.) Exp. 2 (day 20), c.) Exp. 3 (day 14) and d.) Exp. 4 (day 34). In Exp. 1 and 4 (a, d) mainly single, small particles are observed, whereas in Exp. 2 and 3 (b, c) mainly agglomerates are visible.

down, and thus not measured. In addition, since the PSD is number based, the small particles weigh just as heavy in the distribution as the larger ones, and there are clearly more small particles than larger ones in terms of numbers. However, the larger ones were more visible in the microscopy picture. From the rough, lumpy edges of the agglomerates it was observed that they were composed of many small individual crystals (see 1000x magnification pictures for more detail in SI Fig. 2). It is very likely that the addition of the sulfidic reactor also influenced the formation of these agglomerates. Yet, from the light microscopy pictures it became clear that the smallest individual particles were hardly present in Exp. 2 and only to some extent in Exp. 3. Therefore, as a result of the dissolution of the smallest particles, and the enhanced agglomeration observed by addition of the sulfidic reactor, we measured a larger particle size in the gas-lift reactor. In Mol et al. (2021) we elaborated on the agglomeration mechanism. The agglomeration is a result of the balance between dissolution and formation of elemental sulfur.

It is argued that a potential change in biomass composition did not affect the sulfur particle properties. We reported the hydraulic retention times (HRT) of the total reactor set-up in SI Table 1. Hereby we assume that the mean cell residence time (MCRT) is equal to the HRT as the biomass is suspended. For example, Exp.1 and 2 had similar HRTs (8 and 12 days) and durations (31 and 28 days) but the sulfur particle properties were very different. In another publication (Mol et al., 2021) we show similar experiments where we followed the relative abundance of species in the reactor, and we did not see a large change in composition, whereas the properties of the sulfur particles did change within the measured timeframe. In another study it was shown that after 73 days of operation, the biomass composition did change, whereas this change was not yet visible after 19 days (De Rink et al., 2019).

### 3.3. Role of polysulfide formation in removal of the smallest particles

The removal of the smallest particles in the experiments was likely due to the formation of polysulfides in the sulfidic reactor. During the SuRT, sulfur reacted with dissolved bisulfide, and an equilibrium is established with polysulfides (Eq. (7)).

$$HS^- + S_8 \leftrightarrows HS_9^- \leftrightarrows S_9^{2-} + H^+ \quad (7)$$

$$S_9^{2-} + HS^- \leftrightarrows 2S_5^{2-} + H^+ \quad (8)$$

The long chain polysulfides can rearrange to shorter polysulfides by reacting with another HS- ion (Eq. (8)). Polysulfides are known to have an autocatalytic effect on the rate of sulfur dissolution in aqueous sulfide solutions (Hartler et al., 1967; Kleinjan et al., 2005a). This means that once polysulfide is formed, subsequent formation is accelerated as the polysulfide (like the $HS^-$ ion) can also break open the $S_8$ ring and 'dissolve' the elemental sulfur. The general formula for polysulfide can be described as $S_x^{2-}$. The chain length $x$ can vary between 2 and 9, but at moderately alkaline conditions, chain lengths of 4, 5, and 6 are dominant (Kamyshny et al., 2004; Roman et al., 2014). Polysulfides are yellow to orange (Kamyshny et al., 2006; Kleinjan et al., 2005c). By the yellow color of the sulfidic reactor, it was deduced that indeed polysulfides were formed (SI Fig. 3). The degree to which polysulfide formation takes place in the BD process under halo-alkaline conditions is mainly dependent on the amount of available $HS^-$ and sulfur as well as time under anoxic conditions (Kleinjan et al., 2005a; 2005b). In the conventional process reactor line-up, this condition is only met in the absorber. Often the liquid retention time in the absorber is kept short to ensure proper removal of $H_2S$ from the gas by chemical absorption in the mildly alkaline solution. Thus, polysulfide formation takes place only in moderate amounts in the current BD process under halo-alkaline conditions (Roman et al., 2014). However, polysulfide formation should be stimulated as we hypothesize that its formation dissolves the small non-settleable sulfur particles.

To verify whether our observations fit with known thermodynamic and previously reported kinetic data on polysulfide formation (Kamyshny et al., 2004; Kleinjan et al., 2005a;2005b), we created a mathematical model to assess the obtained data. The model inputs were the volume based average PSD of the four experiments and the operational conditions under which these particles were produced (Fig. 6 and

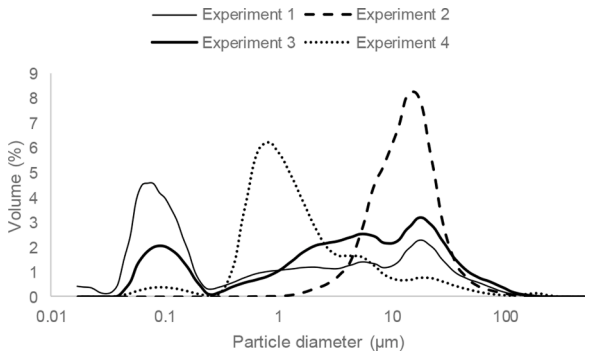


**Fig. 6.** Average volume-based PSD of all four experiments.

SI Table 3). The PSD data was not from the experiments in steady-state phase, but were averages of collected PSD data along the course of the experiments.

From these PSDs, the volume fraction of particles with a diameter <1 μm was calculated. By multiplying this volume fraction by the average measured concentration of elemental sulfur in the experiments, the total concentration of particles <1 μm was calculated. Then, three outputs were calculated: the percentage of $S^0$ that could be converted to $S_x^{2-}$ under the specific conditions from the volume fraction of particles <1 μm, the percentage of $S_x^{2-}$ that could be formed out of the maximal $S_x^{2-}$ concentration at equilibrium and the absolute concentration of $S_x^{2-}$ that could be formed (Fig. 7).

Our modeling results support the experimentally obtained findings that the smallest sulfur particles dissolve in the sulfidic zone, due to polysulfide formation, to the extent allowed by the conditions. Equilibrium between sulfur, TDS and polysulfide was reached for Exp. 2, 3 and 4 (Fig. 7, gray bars). From the model calculations it can thus be concluded that a longer SuRT would not have led to more polysulfide formation for these experiments. In the same way, it is not expected that a longer SuRT would lead to more particle dissolution. In Exp. 1 little polysulfide formation was expected due to the short SuRT, which agrees with the large amount of submicron particles found in the corresponding laboratory experiment. These particles would have been the ones most prone to react to polysulfide, due to their high surface-to-volume ratio. Exp. 2 was the only experiment in which sulfur particles with a diameter <1 μm were nearly absent in the end product. It means that if particles with a diameter < 1 μm were formed somewhere in the process, they are all dissolved in the sulfidic reactor. The model results also supported this finding as 100% of the $S^0$ present in particles < 1 μm could be converted to $S_x^{2-}$. As one of the model assumptions is that sulfur was present in excess, we calculated, under the process conditions of Exp. 2, the maximum capacity of dissolving sulfur particles. While in total 0.93 mg $L^{-1}$ of particles with a size <1 μm was present in the gas-lift reactor, 128 mg $L^{-1}$ of particles could be dissolved when polysulfide

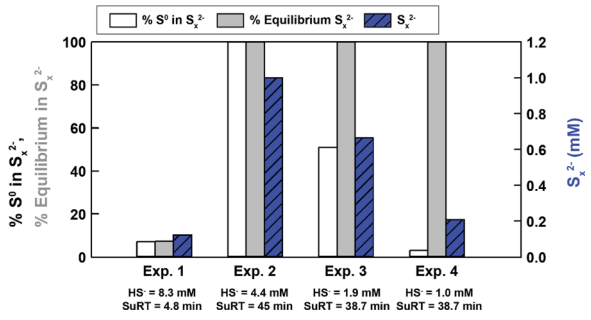


**Fig. 7.** Modelled concentrations of% of S° from particles <1 μm in Sx2− (white bars),% of Sx2− that is in equilibrium with HS− and S0 (gray bars) and absolute Sx2− formed in the sulfidic reactor (blue, diagonally striped bars).

concentrations reached equilibrium. This is almost 140 times more sulfur which could be dissolved in Exp. 2. Consequently, more than 0.93 mg $L^{-1}$ sulfur dissolved, and this probably led to the dissolution of some larger particles. Hence, the model agrees with the experimental data that almost all small particles were dissolved in this experiment. Although equilibrium is reached in Exp. 3 and 4, the model predicted that not enough sulfide was present to dissolve all submicron sulfur particles. This was also shown with the experimental data, as in these experiments submicron particles were still present.

### 3.3.1. *Sensitivity analysis*

In addition to experimental validation, we performed a model simulation to explore the effects of typical operational parameters on polysulfide formation in the BD process. The main factors that we identified to be the most influential on polysulfide formation are:

1.) Sulfidic retention time (SuRT): sufficient time in an oxygen-free environment is needed to reach the equilibrium between TDS, sulfur and polysulfide and consequently the maximum achievable polysulfide concentration (Kleinjan et al., 2005a).

2.) Total dissolved sulfide concentration: the higher the concentration, the more polysulfide can be formed (assuming elemental sulfur is in abundance) and the faster the equilibrium is reached due to the autocatalytic effect of polysulfide formation (Hartler et al., 1967). In this study, the $S^0$:$HS^-$ ratio was different in each experiment. The $S^0$:$HS^-$ ratios were 1.6, 6.7, 33.7 and 63.8 for Exp.1–4 respectively based on the TDS concentration in the sulfidic zone (Table 1) and elemental sulfur concentration (SI Table 1) . However, in Exp.1, equilibrium was not reached, which means that not all of the polysulfide that potentially could be formed under the given ratio indeed was formed.

3.) Particle size: the smaller the particles, the more rapid the formation of polysulfides is due to the higher specific surface area (Kleinjan et al., 2005a).

4.) pH: the higher the pH, the more the equilibrium between total dissolved sulfide and polysulfides shifts towards polysulfides (Kleinjan et al., 2005b; Van Den Bosch et al., 2008). In our study, the pH was kept constant at around 8.5 and therefore it is expected not to have influenced the outcome of this study.

5.) Temperature: a higher temperature will lead to more rapid polysulfide formation (Kamyshny et al., 2004; Kleinjan et al., 2005a). However, the temperature limit for the BD process is around 40 °C. Above 45 °C irreversible thermal inactivation of the SOB occurs (De Rink et al., 2020). On the other hand, if the temperature is too low (i.e. below 25 °C), the metabolism of the SOB will be reduced such that not enough activity remains to carry out desulfurization adequately. In our experiments, temperature was kept constant at around 35 °C and therefore is not expected to have influence the results.

As an example, we show the simulation of the dependency of two parameters (TDS and SuRT) on the steady state polysulfides concentration in a CSTR under sulfidic conditions, assuming all other parameters remain constant (Fig. 8). We choose these parameters as they have most potential for adjustment in the current process during operation. The polysulfide concentration in steady state depends proportionally on the TDS concentration (Fig. 8A). At the highest concentration of TDS (4 mM), the highest polysulfide concentration is reached (close to 1 mM). This in turn affects the amount of sulfur that can be dissolved to polysulfide. The more sulfur is dissolved, the more likely it will be that all poorly settleable particles are dissolved. The SuRT at which polysulfide equilibrium concentrations are reached also strongly depends on the total dissolved sulfide concentration: the higher the concentration, the quicker the equilibrium is reached (Fig. 8B). This pattern does not show a proportional effect. In contrast, the lower the TDS concentration in the sulfidic reactor, the exponentially longer it takes to reach equilibrium. This can be attributed to the autocatalytic effect of polysulfide formation described earlier.

For the BD process, it can thus be concluded that two variables are the most important for sulfur particle dissolution: how much polysulfide

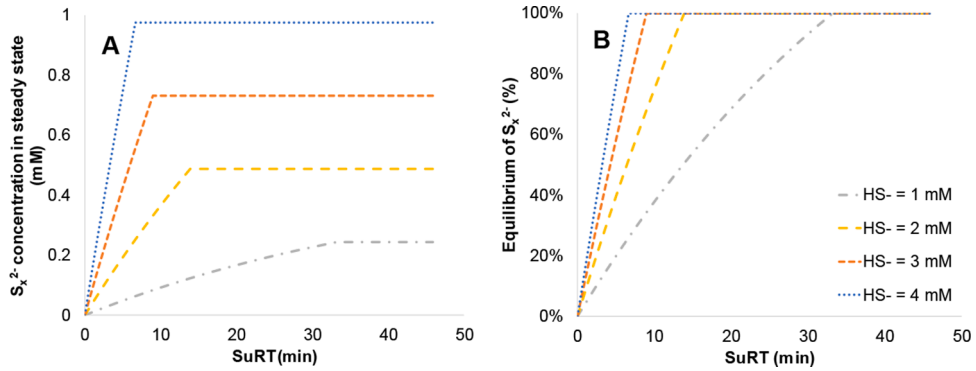


**Fig. 8.** A: Polysulfide concentration in steady state as function of total sulfide concentration and SuRT, B: Equilibrium of polysulfide concentration as function of total sulfide concentration and SuRT.

will be formed at equilibrium and the rate at which equilibrium is reached. The amount of polysulfide that will be formed is mainly dependent on the TDS concentration and, when equilibrium is not reached, SuRT (assuming equal pH and temperature). The rate at which equilibrium is reached is mainly influenced by TDS (assuming equal temperature). One would expect a higher formation of thiosulfate due to chemical oxidation of the increased polysulfide concentration. However, it was shown by de Rink et al. (2019) that addition of the sulfidic reactor did not lead to extra thiosulfate formation. The product selectivity for thiosulfate was only 2.0%. The thiosulfate selectivity in our experiments was also not significantly different between experiments and on average below 4.3%. In addition, Avetisyan et al. (2021) showed that at pH 8.5 chemically almost no thiosulfate was formed. Based on these results it is hypothesized that the oxidation of polysulfide is not chemical but biological, hence not leading to thiosulfate formation (Eq. (9))

$$S_x^{2-} + 1/2O_2 + H^+ \rightarrow xS^0 + OH^- \quad (9)$$

This reaction also ensures that polysulfide formation itself as shown in Eqs. (7) and 8 does not lead to an overall acidification and thus is pH neutral.

### 3.4. Future research

Sulfur is a strongly hydrophobic, molecular crystal with extremely low solubility (5 μg $L^{-1}$) (Boulègue, 1978), which makes its crystallization quite complex to study, especially in continuous, biological reactor systems where local sulfur concentrations may vary. As shown in our experiments, the polysulfide formation in the sulfidic reactor leads to a substantial amount of sulfur dissolution. This means that in the BD process, not only sulfur particle formation is important for the particle size distribution, but also the particle dissolution. However, the sulfur which has been 'dissolved' to polysulfides, is oxidized (again) once it reaches the gas-lift reactor, and thereby sulfur is produced again. To understand this process better, polysulfide concentration and speciation should be determined during reactor experiments. Furthermore, in relation to polysulfide formation, it should be investigated what the boundary conditions are to remove of the smallest sulfur particles and to produce large enough agglomerates for proper settling. This could be achieved by experiments varying the S0:$HS^-$ ratio and SuRT, but modeling work could also help to predict what these boundary conditions would be.

## 4. Conclusion

In this paper, we investigated the effect of the addition of a sulfidic reactor on the properties of sulfur particles formed in the BD process. With this novel process design the smallest particles (<1 μm) were dissolved to polysulfides. This almost complete removal of particles only occurred when the SuRT was long enough to reach polysulfide equilibrium concentration and when TDS levels were sufficiently high that enough polysulfide could be formed. These results have great implications from an engineering perspective. Model calculations with thermodynamic and kinetic data on polysulfide formation support the experimental findings. The novel line-up is thus a promising reactor configuration that allows for improved sulfur recovery due to the removal of the smallest sulfur particles.

Annemerel Mol reports financial support was provided by Paqell BV.

## Funding

This work was financially supported by Paqell B.V.

## Declaration of Competing Interest

The authors declare that they have no known competing financial interests or personal relationships that could have appeared to influence the work reported in this paper.

## Data Availability

Data will be made available on request.

## Acknowledgements

We would like to thank the members of the Wetsus Sulfur Theme and the ETE-MIB sulfur thesis ring for the fruitful discussions.

## Supplementary materials

Supplementary material associated with this article can be found, in the online version, at doi:10.1016/j.watres.2022.119296.

## References

Avetisyan, K., Zweig, I., Luther, G.W., Kamyshny, A., 2021. Kinetics and mechanism of polysulfides and elemental sulfur formation by a reaction between hydrogen sulfide and δ-MnO2. Geochim. Cosmochim. Acta 313, 21–37. https://doi.org/10.1016/j.gca.2021.08.022.

Boulègue, J., 1978. Solubility of elemental sulfur in water at 298K. Phosphorus Sulfur Relat. Elem. 5, 127–128.

Buisman, C.J., Geraats, B.G., Ijspeert, P., Lettinga, G., 1990. Optimization of sulphur production in a biotechnological sulphide-removing reactor. Biotechnol. Bioeng. 35, 50–56. https://doi.org/10.1002/bit.260350108.

Cline, C., Hoksberg, A., Abry, R., Janssen, A.J.H., 2003. Biological process for H2S removal from gas streams the shell-paques/thiopaqtm gas desulfurization process 23–26.

De Rink, R., Klok, J.B.M., Heeringen, G.J.Van, Keesman, K.J., 2020. Biologically enhanced hydrogen sulfide absorption from sour gas under haloalkaline conditions. J. Hazard. Mater. 383, 121104 https://doi.org/10.1016/j.jhazmat.2019.121104.

De Rink, R., Klok, J.B.M., Heeringen, G.J.Van, Sorokin, D.Y., Heijne, A., Zeijlmaker, R., Mos, Y.M., Wilde, V.De, Keesman, K.J., Buisman, C.J.N., 2019. Increasing the selectivity for sulfur formation in biological gas desulfurization. Environ. Sci. Technol. 53, 4519–4527. https://doi.org/10.1021/acs.est.8b06749.

Di Capua, F., Ahoranta, S.H., Papirio, S., Lens, P.N.L., Esposito, G., 2016. Impacts of sulfur source and temperature on sulfur-driven denitrification by pure and mixed cultures of Thiobacillus. Process Biochem 51, 1576–1584. https://doi.org/10.1016/j.procbio.2016.06.010.

Eriksen, J., Thorup-kristensen, K., Askegaard, M., 2004. Plant availability of catch crop sulfur following spring incorporation. J.Plant Nutr. Soil. Sci. 609–615. https://doi.org/10.1002/jpln.200420415.

Field, A., 2009. 1.7.2.2. The median, in: Discovering Statistics Using SPSS. SAGE Publications Ltd., London, pp. 21–22.

Florentino, A.P., Weijma, J., Stams, A.J.M., Sánchez-Andrea, I., 2015. Sulfur reduction in acid rock drainage environments. Environ. Sci. Technol. 49, 11746–11755. https://doi.org/10.1021/acs.est.5b03346.

Guidotti, T.L., 2010. Hydrogen sulfide: advances in understanding human toxicity. Int. J. Toxicol. 29, 569–581. https://doi.org/10.1177/1091581810384882.

Hartler, N., Libert, J., Teder, A., 1967. Rate of sulfur dissolution sodium sulfide in aqueous sodium sulfide. Ind. Eng. Chem. Process Des. Dev. 6, 398–406. https://doi.org/10.1021/i260024a002.

Janssen, A.J.H., De Keizer, A., Van Aelst, A., Fokkink, R., Yangling, H., Lettinga, G., 1996. Surface characteristics and aggregation of microbiologically produced sulphur particles in relation to the process conditions. Colloids Surfaces B Biointerfaces 6, 115–129. https://doi.org/10.1016/0927-7765(95)01246-X.

Janssen, A.J.H., Lens, P.N.L., Stams, A.J.M., Plugge, C.M., Sorokin, D.Y., Muyzer, G., Dijkman, H., Van Zessen, E., Luimes, P., Buisman, C.J.N., 2009. Application of bacteria involved in the biological sulfur cycle for paper mill effluent purification. Sci. Total Environ. 407, 1333–1343. https://doi.org/10.1016/j.scitotenv.2008.09.054.

Janssen, A.J.H., Lettinga, G., Keizer, A.De, 1999. Removal of hydrogen sulphide from wastewater and waste gases by biological conversion to elemental sulphur colloidal and interfacial aspects of biologically produced sulphur particles 151, 389–397.

Kamyshny, A., Ekeltchik, I., Gun, J., Lev, O., 2006. Method for the determination of inorganic polysulfide distribution in aquatic systems 78, 2631–2639. https://doi.org/10.1021/ac051854a.

Kamyshny, A., Gun, J., Rizkov, D.A.N., Voitsekovski, T., Lev, O., 2004. Equilibrium distribution of polysulfide ions in aqueous solutions at different temperatures by rapid single phase derivatization. Environ. Sci. Technol. 41, 2395–2400.

Kiragosyan, K., Klok, J.B.M., Keesman, K.J., Roman, P., Janssen, A.J.H., 2019. Development and validation of a physiologically based kinetic model for starting up and operation of the biological gas desulfurization process under haloalkaline conditions. Water Res. X 4, 100035. https://doi.org/10.1016/j.wroa.2019.100035.

Kiragosyan, K., Picard, M., Sorokin, D.Y., Dijkstra, J., Klok, J.B.M., Roman, P., Janssen, A.J.H., 2020. Effect of dimethyl disulfide on the sulfur formation and microbial community composition during the biological H 2 S removal from sour gas streams. J. Hazard. Mater. 386, 121916 https://doi.org/10.1016/j.jhazmat.2019.121916.

Kleinjan, W.E., Keizer, A.De, Janssen, A.J.H., 2005a. Kinetics of the Reaction between Dissolved Sodium Sulfide and Biologically Produced Sulfur. Ind. Eng. Chem. Res. 44, 309–317.

Kleinjan, W.E., Keizer, A.De, Janssen, A.J.H., 2005b. Equilibrium of the reaction between dissolved sodium sulfide and biologically produced sulfur 43, 228–237. https://doi.org/10.1016/j.colsurfb.2005.05.004.

Kleinjan, W.E., Keizer, A.De, Janssen, A.J.H., 2005c. Kinetics of the chemical oxidation of polysulfide anions in aqueous solution 39, 4093–4100. https://doi.org/10.1016/j.watres.2005.08.006.

Kleinjan, W.E., Marcelis, C.L.M., De Keizer, A., Janssen, A.J.H., Stuart, M.A.C., 2006. Foam formation in a biotechnological process for the removal of hydrogen sulfide from gas streams. Colloids Surfaces A Physicochem. Eng. Asp. 275, 36–44. https://doi.org/10.1016/j.colsurfa.2005.09.015.

Klok, J.B., van Heeringen, G., De Rink, R., Wijnbelt, H., 2017. Introducing the next generation of the THIOPAQ O&G process for biotechnological gas desulphurization: THIOPAQ-SQ. Sulphur.

Klok, J.B.M., de Graaff, M., van den Bosch, P.L.F., Boelee, N.C., Keesman, K.J., Janssen, A.J.H., 2013. A physiologically based kinetic model for bacterial sulfide oxidation. Water Res. https://doi.org/10.1016/j.watres.2012.09.021.

Klok, J.B.M., Van Den Bosch, P.L.F., Buisman, C.J.N., Stams, A.J.M., Keesman, K.J., Janssen, A.J.H., 2012. Pathways of sulfide oxidation by haloalkaliphilic bacteria in limited-oxygen gas lift bioreactors. Environ. Sci. Technol. 46, 7581–7586. https://doi.org/10.1021/es301480z.

Leerdam, R.C.Van, Bosch, P.L.F.Van Den, Lens, P.N.L., Janssen, A.J.H., 2011. Reactions between methanethiol and biologically produced sulfur particles 1320–1326. https://doi.org/10.1021/es102987p.

Li, W., Zhang, M., Kang, D., Chen, W., Yu, T., Xu, D., Zeng, Z., Li, Y., 2020. Mechanisms of sulfur selection and sulfur secretion in a biological sulfide removal (BISURE) system Mechanisms of sulfur selection and sulfur secretion in a biological sul fi de removal (BISURE) system. Environ. Int. 137, 105549 https://doi.org/10.1016/j.envint.2020.105549.

Likens, G.E., Bormann, F.H., 1974. Acid rain : a serious regional environmental problem. Science 184, 1176–1179, 80-.

Lim, J., Pyun, J., Char, K., 2015. Recent approaches for the direct use of elemental sulfur in the synthesis and processing of advanced materials. Angew. Chemie - Int. Ed. 54, 3249–3258. https://doi.org/10.1002/anie.201409468.

Marnocha, C.L., Levy, A.T., Powell, D.H., Hanson, T.E., Chan, C.S., 2016. Mechanisms of extracellular S 0 globule production and degradation in Chlorobaculum tepidum via dynamic cell – globule interactions. Microbiology 162, 1125–1134. https://doi.org/10.1099/mic.0.000294.

Mol, A.R., Langeveld, L.J.van, Weijden, R.D.van der, Klok, J.B.M., Buisman, C.J.N., 2022. Effect of Sulfide on Morphology and Particle Size of Biologically Produced Elemental Sulfur from Industrial Desulfurization Reactors. J. Hazard. Mater. 424, 127696 https://doi.org/10.1016/j.jhazmat.2021.127696.

Mol, A.R., Meuwissen, D.J.M., Pruim, S.D., Zhou, C., Vught, V.van, Klok, J.B.M., Buisman, C.J.N., Weijden, R.D.van der, 2021. Novel Agglomeration Strategy for Elemental Sulfur Produced during Biological Gas Desulfurization. ACS Omega 6. https://doi.org/10.1021/acsomega.1c03701, 27913–27323.

Mol, A.R., Weijden, R.D.Van Der, Klok, J.B.M., Buisman, C.J.N., 2020. Properties of Sulfur Particles Formed in Biodesulfurization of. Biogas. Minerals 10. https://doi.org/10.3390/min10050433.

Mu, T., Yang, M., Xing, J., 2021. Performance and characteristic of a haloalkaliphilic biodesulfurizing system using Thioalkalivibrio verustus D301 for efficient removal of H 2 S. Biochem. Eng. J. 165, 107812 https://doi.org/10.1016/j.bej.2020.107812.

Palme, H., Lodders, K., Jones, A., 2014. Solar system abundances of the elements, in: Davis, A.M. (Ed.), Planets, Asteroids, Comets and The Solar System, Volume 2 of the Treatise of Geochemistry. Elsevier, pp. 15–36. https://doi.org/10.1007/978-3-642-10352-0_8.

Pfennig, N., Lippert, K.D., 1966. Uber das Vitamin B12-bedurfnis phototropher Schwefelbacterien. Arch. Microbiol. 55, 245–256. https://doi.org/10.1007/BF00410246.

Pope, C.A., Rodermund, D.L., Gee, M.M., 2007. Mortality effects of a copper smelter strike and reduced ambient sulfate particulate matter air pollution. Environ. Health Perspect. 115, 679–683. https://doi.org/10.1289/ehp.9762.

Roig, A., Cayuela, M.L., Sa, M.A., 2004. The use of elemental sulphur as organic alternative to control pH during composting of olive mill wastes 57, 1099–1105. https://doi.org/10.1016/j.chemosphere.2004.08.024.

Roman, P., 2016. Biotechnological Removal of H2S and Thiols from Sour Gas Streams Under Haloalkaline Conditions. Wageningen University.

Roman, P., Bijmans, M.F.M., Janssen, A.J.H., 2014. Quantification of individual polysulfides in lab-scale and full-scale desulfurisation bioreactors. Environ. Chem. 11, 702. https://doi.org/10.1071/en14128.

Seidel, H., Wennrich, R., Hoffmann, P., Löser, C., 2006. Effect of different types of elemental sulfur on bioleaching of heavy metals from contaminated sediments. Chemosphere 62, 1444–1453. https://doi.org/10.1016/j.chemosphere.2005.06.003.

Smith, S.J., Van Aardenne, J., Klimont, Z., Andres, R.J., Volke, A., Delgado Arias, S., 2011. Anthropogenic sulfur dioxide emissions, 1850-2005 Atmos. Chem. Phys. 11, 1101–1116. https://doi.org/10.5194/acp-11-1101-2011.

Soares, M.I.M., 2002. Denitrification of groundwater with elemental sulfur. Water Res 36, 1392–1395. https://doi.org/10.1016/S0043-1354(01)00326-8.

Sorokin, D.Y., Zhilina, T.N., Lysenko, A.M., Tourova, T.P., Spiridonova, E.M., 2006. Metabolic versatility of haloalkaliphilic bacteria from soda lakes belonging to the Alkalispirillum-Alkalilimnicola group. Extremophiles 10, 213–220. https://doi.org/10.1007/s00792-005-0487-7.

Ucar, D., Yilmaz, T., Di Capua, F., Esposito, G., Sahinkaya, E., 2020. Comparison of biogenic and chemical sulfur as electron donors for autotrophic denitrification in sulfur-fed membrane bioreactor (SMBR). Bioresour. Technol. 299, 122574 https://doi.org/10.1016/j.biortech.2019.122574.

Van Den Bosch, P.L.F., Sorokin, D.Y., Buisman, C.J.N., Janssen, A.J.H., 2008. The effect of pH on thiosulfate formation in a biotechnological process for the removal of hydrogen sulfide from gas streams. Environ. Sci. Technol. https://doi.org/10.1021/es7024438.

Van Den Bosch, P.L.F., Van Beusekom, O.C., Buisman, C.J.N., Janssen, A.J.H., 2007. Sulfide oxidation at halo-alkaline conditions in a fed-batch bioreactor. Biotechnol. Bioeng. 97, 1053–1063. https://doi.org/10.1002/bit.21326.

Zhu, T.T., Cheng, H.Y., Yang, L.H., Su, S.G., Wang, H.C., Wang, S.Sen, Wang, A.J., 2019. Coupled Sulfur and Iron(II) carbonate-driven autotrophic denitrification for significantly enhanced nitrate removal. Environ. Sci. Technol. 53, 1545–1554. https://doi.org/10.1021/acs.est.8b06865.